



Published in final edited form as:

*J Muscle Res Cell Motil.* 2020 September ; 41(2-3): 221–237. doi:10.1007/s10974-019-09568-0.

## **$\beta$ -guanidinopropionic acid and metformin differentially impact autophagy, mitochondria and cellular morphology in developing C2C12 muscle cells**

**Chelsea L. Crocker<sup>1</sup>, Bradley L. Baumgarner<sup>2</sup>, Stephen T. Kinsey<sup>1</sup>**

<sup>1</sup>Department of Biology and Marine Biology, University of North Carolina Wilmington, Wilmington, NC 28403, USA

<sup>2</sup>Division of Natural Sciences and Engineering, University of South Carolina Upstate, Spartanburg, SC 29303, USA

### **Abstract**

The serine/threonine kinase AMP-activated protein kinase (AMPK) is a drug target for the treatment of obesity and type 2 diabetes (T2D). Metformin, a widely prescribed anti-hyperglycemic agent, and  $\beta$ -guanidinopropionic acid ( $\beta$ -GPA), a dietary supplement and creatine analog, have been shown to increase activity of AMPK. Macroautophagy is an intracellular degradation pathway for aggregated proteins and dysfunctional organelles, which can be mediated by AMPK. The present study sought to elucidate how metformin and  $\beta$ -GPA affect cell morphology, AMPK activity, autophagy and mitochondrial morphology and function in developing C2C12 myotubes.  $\beta$ -GPA reduced myotube diameter and increased length throughout differentiation, while metformin increased myotube diameter only at the 48-h time point.  $\beta$ -GPA treatment enhanced AMPK signaling and expression of autophagy-related proteins.  $\beta$ -GPA treatment also increased the density of autophagosomes, autolysosomes, and lysosomes. Metformin also increased activation of AMPK after 48 h, but in contrast to  $\beta$ -GPA, led to a dramatic reduction in the density of autophagosomes and lysosomes. Both metformin and  $\beta$ -GPA reduced the mitochondrial oxygen consumption rate, and differentially altered mitochondrial morphology. Obesity and T2D have been shown to increase mitochondrial dysfunction and reduce autophagic flux in skeletal muscle cells. Therefore,  $\beta$ -GPA may help to alleviate the effects of metabolic disease by increasing autophagic flux in skeletal muscle cells. In contrast, the reduction of autophagy by metformin may lead to dysregulation of mitochondrial maintenance, as well as muscle development.

### **Keywords**

Autophagy; skeletal muscle; mitochondria; AMPK; metformin;  $\beta$ -guanidinopropionic acid

## Introduction

AMP-activated protein kinase (AMPK) plays a role in the regulation of glucose and lipid metabolism, and has been considered an attractive drug target for the treatment of obesity and type 2 diabetes (T2D) (Winder and Hardie 1999; Zhou, et al. 2001). AMPK is a cellular energy sensor that regulates metabolic homeostasis by responding to cellular energy deficits manifested as changes in the AMP/ATP ratio (Oakhill, et al. 2011; Hardie 2007; Hardie 2005). Such cellular energy deficits are caused by glucose deprivation, oxidative stress, exercise, and muscle contraction (Winder and Hardie 1996; Hutber, Hardie, and Winder 1997; Williamson, Butler, and Alway 2009). Phosphorylation of a threonine residue (Thr<sup>172</sup>) on the catalytic subunit is required for activation of the kinase domain of AMPK (Hawley, et al. 1996). Increased AMPK activity leads to inhibition of hepatic glucose production and increased fatty acid oxidation in the liver and muscle (Merrill, et al. 1997; Hardie, et al. 1999; Foretz, et al. 2010; Zhou, et al. 2001; Suwa, Nakano, and Kumagai 2003). In skeletal muscle, increased AMPK activity results in enhanced insulin sensitivity and increased glucose uptake via increased expression and translocation of the glucose transporter GLUT4 (Holmes, Kurth-Kraczek, and Winder 1999; Kurth-Kraczek, et al. 1999; Winder and Hardie 1999; Iglesias, et al. 2002). Further, chronic activation of AMPK mimics the results of exercise training by increasing mitochondrial turnover (Jager, et al. 2007; Bergeron, et al. 2001; Zong, et al. 2002), and expression of muscle hexokinase (Holmes, Kurth-Kraczek, and Winder 1999). As such, AMPK has been proposed as a drug target with the potential to mediate beneficial effects for the treatment of metabolic conditions such as obesity and T2D (Zhou, et al. 2001; Zhang, Zhou, and Li 2009; Hardie 2003).

Metformin (dimethylbiguanide) is one of the most widely prescribed anti-hyperglycemic and insulin sensitizing agents for the treatment of obesity and T2D (Viollet, et al. 2012; Stumvoll, et al. 1995; Stumvoll, Haring, and Matthaei 2007). The principal glucose lowering effects of metformin are attributed to an inhibition of hepatic glucose production and an increase in glucose utilization in skeletal muscle (Foretz, et al. 2010; Galuska, et al. 1994; Cusi and DeFronzo 1998; Hundal, et al. 2000). It has been suggested that AMPK may mediate many of the beneficial effects of metformin, as metformin has been shown to activate AMPK in hepatocytes and skeletal muscle (Musi, et al. 2002; Zhou, et al. 2001). It has been proposed that activation of AMPK by metformin is a result of an increase in the AMP/ATP ratio caused by mitochondrial stress in the form of electron transport Complex I inhibition (Stephenne, et al. 2011; Fryer, Parbu-Patel, and Carling 2002). The mechanism by which metformin reduces plasma glucose levels remains controversial, as some work has demonstrated LKB1 and AMPK deficient mice treated with metformin still exhibit glucose reduction (Foretz, et al. 2010). However, other work has shown that deletion of LKB1 abolishes the metformin-induced reduction in blood glucose (Shaw, et al. 2005). Similarly, while there are a number of studies that demonstrate metformin-induced inhibition of Complex I, some report that metformin does not alter Complex I in cell free assays (El-Mir, et al. 2000), or in human skeletal muscle (Larsen, et al. 2012). Despite the controversy, many studies agree that metformin inhibits mitochondrial Complex I and activates AMPK (Stephenne, et al. 2011; Ota, et al. 2009). It has also been suggested that

AMPK may mediate the long-term insulin-sensitizing effects of metformin (Rena, Hardie, and Pearson 2017).

In skeletal muscle, creatine kinase catalyzes the transfer of a high-energy phosphate between creatine and ADP, forming phosphocreatine or ATP (Wallimann, et al. 1998). Creatine kinase therefore plays an important role in skeletal muscle ATP synthesis.  $\beta$ -guanidinopropionic acid ( $\beta$ -GPA) is a creatine analog that competitively inhibits cellular creatine uptake (Shields and Whitehair 1973; Fitch, et al. 1975). This in turn leads to the depletion of cellular creatine, phosphocreatine, and ATP levels, and reduces the cell's ability to buffer ATP concentration during increases in ATP demand (Fitch, Jellinek, and Mueller 1974; Shoubridge, et al. 1985). Dietary  $\beta$ -GPA supplementation reduces skeletal muscle mass and body mass (Williams, et al. 2009; Baumgarner, et al. 2015; Roussel, et al. 2000). In addition,  $\beta$ -GPA has been shown to enhance endurance capacity and fatigue resistance in skeletal muscle, which is accompanied by shifts toward more oxidative fiber types (Ohira, et al. 2003; Ren, et al. 1995; Wakatsuki, et al. 1995). Studies have also demonstrated that  $\beta$ -GPA leads to increases in mitochondrial oxidative enzymes, mitochondrial biosynthesis (Reznick and Shulman 2006; Reznick, et al. 2007), and fatty acid oxidation (Pandke, et al. 2008). Additionally,  $\beta$ -GPA increases skeletal muscle glucose uptake and enhances insulin sensitivity (Ohira, et al. 1994). Many of these effects are attributed to the activation of AMPK, which is a direct result of the reduced cellular ATP levels (Rush, Tullson, and Terjung 1998).

The activation of AMPK is associated with inhibition of protein synthesis and enhanced protein degradation via the ubiquitin-proteasome system and the autophagy-lysosomal system (Gwinn, et al. 2008; Egan, et al. 2011). Macroautophagy (hereafter referred to simply as autophagy) is a highly conserved intracellular degradation pathway for nutrient recycling. Autophagy is characterized by the engulfment of cellular material such as aggregated proteins and dysfunctional organelles, followed by lysosomal fusion and degradation (Levine and Klionsky 2004; Kim and Klionsky 2000). Autophagy is constitutively active at a basal level in most tissues, but it also can be induced by low cellular energy levels or shifts in nutrient availability (Kim and Lee 2014). AMPK and the mechanistic target of rapamycin complex 1 (mTORC1) play a significant role in autophagy regulation. In addition to autophagy, mTORC1 is involved in regulation of cell growth, protein synthesis, and lipogenesis (Laplante and Sabatini 2009; Wullschleger, Loewith, and Hall 2006; Hay and Sonenberg 2004). The autophagy initiating kinase UNC-51-like kinase 1 (ULK1) forms a complex with three other autophagy related proteins, FIP200, ATG13, and ATG101 (Jung et al. 2009). When nutrients are plentiful, mTORC1 phosphorylates the ULK1 complex, inhibiting autophagy (Hosokawa, et al. 2009). When nutrients are limited, mTORC1 is inhibited, the ULK1 complex dissociates from mTORC1, and autophagy is initiated (Jung, et al. 2009; Ganley, et al. 2009). AMPK activates autophagy by inhibiting mTORC1 and directly phosphorylating ULK1 at a different site than mTORC1 (Kim, et al. 2011; Egan, et al. 2011). Vesicle elongation is mediated by several autophagy proteins, including microtubule-associated protein 1 light chain 3 (LC3), which exists in a cytosolic form (LC3-I) and a form associated with the autophagosome membrane (LC3-II) (Kabeya, et al. 2000). Nutrients generated from lysosomal degradation reactivate mTORC1, leading to

autophagy termination. Autophagy can be general, or specifically targeted to organelles such as mitochondria, which is referred to as mitophagy (Lemasters 2005).

Mitochondria are highly dynamic organelles that can vary morphologically from symmetrical spheres to an interconnected network (Bereiterhahn and Voth 1994). These morphological alterations are regulated by mitochondrial fission and fusion. Fission and fusion dynamics, and subsequent mitochondrial morphology, are influenced by a number of factors including nutrient availability and cellular stress (Chan 2006; Yu, Rotherham, and Yoon 2006). Mitochondrial dysfunction can lead to insulin resistance, a primary risk factor for obesity and T2D (Morino, Petersen, and Shulman 2006). In skeletal muscle of obese and T2D individuals, mitochondrial dysfunction is accompanied by morphological changes, such as reduced size (Kelley, et al. 2002). Agents that alter energy status and mitochondrial function, such as metformin and  $\beta$ -GPA, may lead to changes in mitochondrial morphology and autophagy in muscle. Further, autophagy and mitochondrial function have been implicated as potential therapeutic targets for metabolic disease (Jheng, et al. 2012; Rubinsztein, Codogno, and Levine 2012). While metformin and  $\beta$ -GPA have been shown to alter skeletal muscle metabolism, it remains unclear how these pharmacological agents affect autophagy and mitochondrial function.

The primary objective of this study was to investigate how metformin and  $\beta$ -GPA treatment affects autophagy in developing myotubes. Since the AMPK/mTORC1 pathway plays an important role in autophagy regulation, relative expression of key proteins in this pathway were examined. Similarly, given that autophagy and AMPK activity are associated with various cellular stressors, myotube morphology, mitochondrial morphology, and mitochondrial function were also examined. Since both  $\beta$ -GPA and metformin have been shown to cause energetic stress and activate the AMPK signaling pathway, we hypothesized that after short-term (48 h) treatment, both  $\beta$ -GPA and metformin: 1) will decrease myotube diameter, 2) will increase AMPK phosphorylation, 3) will enhance autophagy, 4) will increase mitochondrial fragmentation, since mitochondrial fission precedes mitophagy, and 5) will reduce the cellular oxygen consumption rate. These hypotheses were all supported following  $\beta$ -GPA treatment. In contrast, while metformin did lead to an increase in AMPK phosphorylation and a decrease in the oxygen consumption rate, it also led to an increase in myotube diameter, a decrease in autophagy, and elongation of mitochondria instead of increased fission. Thus, these two AMPK activating compounds have fundamentally different effects on autophagy.

## Methods and Materials

### Cell culture

C2C12 mouse myoblasts were purchased from ATCC (Manassas, VA, USA) and cultured in growth media comprised of Dulbecco's modified eagle medium (DMEM, high (25 mM) glucose, GlutaMAX supplement, pyruvate) (Life technologies, Carlsbad, CA, USA) supplemented with 10% fetal bovine serum and 1% penicillin/streptomycin. Cells were grown to <70% confluence in 75 cm<sup>2</sup> culture flasks (Sigma-Aldrich, Natick, MA, USA), and maintained in a Nuair air-jacketed incubator at 37°C and 5% CO<sub>2</sub>. Cells were passaged using TrypLE Express (Life technologies). Following seeding, cells remained in

growth media for 24 h, and were subsequently switched to differentiation media (DM) (DMEM, 2% horse serum, and 1% penicillin/streptomycin) to promote differentiation of mononucleated myoblasts to multinucleated myotubes. Metformin or  $\beta$ -GPA treated cells were supplemented with either 1 mM metformin or 5 mM  $\beta$ -GPA when GM was replaced with DM.

### Myotube measurements

Cells were seeded in 6-well plates (Corning, NY, USA) at a density of 200,000 cells per well and cultured as described above. Phase-contrast images were captured each day, starting at 48 h post-treatment. Three images were taken per well, one in the middle, one in the top right, and one in the bottom left. This was conducted for four plates ( $n=12$ ), each day of treatment for five days, resulting in 36 images per treatment type (control, metformin, or  $\beta$ -GPA) per day, and each developing myotube in the frame was measured using FIJI (Schindelin, et al. 2012).

### Western blot analysis

Cells were seeded into 6-well plates at a density of 200,000 cells per well and cultured as described above. Cells were lysed using radioimmunoprecipitation assay (RIPA) buffer (Santa Cruz Biotechnology, Dallas, TX, USA) with 10 $\mu$ l/ml of Na-orthovanadate, PMSF, and protease inhibitor. Samples were centrifuged at 12,000 rpm for 20 min at 4°C and the supernatants were collected. Protein content was quantified using a Bradford assay. Lysates were combined with 2x Laemmli buffer in a 1:1 ratio, denatured for 5min and 10–15  $\mu$ g of protein was loaded into a 10% SDS polyacrylamide gel (Bio-Rad, Hercules, CA, USA). Proteins were transferred to a PVDF membrane at approximately 250 mA for 1 h using a wet transfer technique. Membranes were washed 2x in Tris-buffered saline with 0.1% Tween 20 (TBST), and blocked in 3% milk or BSA in TBST for 1 h. Membranes were incubated in 3% milk or BSA with the primary antibody (in a 1:1000 dilution) at 4°C overnight. Membranes were washed in TBST 4x for 5 min, incubated in an HRP-linked secondary antibody (1:2000 dilution) in 3% milk or BSA for 1 h, and rinsed in TBST 4x for 5 min. Blots were incubated for 5 min in an enhanced chemiluminescent (ECL) substrate (Bio-Rad) and imaged using a CCD camera. Following detection, membranes were stained for total protein using Coomassie Brilliant Blue R-250 for 5 min, de-stained, and rinsed with DI H<sub>2</sub>O. Densitometry was conducted using FIJI, by selecting each lane and analyzing the area under each peak. The following antibodies (Cell Signaling Technology, Danvers, MA, USA) were used LC3B (#83506S), ULK1 (#8054), Phospho-ULK1 (Ser<sup>317</sup>), AMPK (#2532), Phospho-AMPK (Thr<sup>172</sup>) (#40H9), Phospho-p70 S6 Kinase (Thr<sup>389</sup>) (#9205), and p70 S6 kinase (#9202).

### Fluorescence microscopy

Cells were seeded into collagen-coated coverslip dishes (MatTek, Ashland, MA, USA), and stained with 50 nM LysoTracker Red DND-99 (Life technologies, Carlsbad, CA, USA) in DM for 30 min in a CO<sub>2</sub> air-jacketed incubator at 37°C and 5% CO<sub>2</sub>. Cells were washed in phosphate-buffered saline (PBS) 2x, fixed in 4% paraformaldehyde for 15 min, and stained with DAPI for 20 min at 37°C. All samples were permeated with 0.5% Triton X-100 in PBS for 15 min and blocked in 0.5% BSA in PBS for 1 h at room temperature. Samples were

incubated in 1:500 dilution of LC3B primary antibody (Cell Signaling; #83506S) in 0.25% BSA in PBS for 1 h at room temperature, washed 3x with PBS, and incubated in 0.25% BSA in PBS with an Alexa Fluor 488 conjugated secondary antibody in a 1:4000 dilution (Abcam, Cambridge, UK) for 1 h at room temperature. Imaging was conducted on an Olympus Fluoview 1000 laser scanning confocal microscope. Fifteen images were collected from each coverslip ( $n=3$ ), and images were analyzed in FIJI. Density was calculated as a ratio of the number of LC3-II or lysosome puncta to the number of nuclei in each image frame.

### Transmission electron microscopy

Cells were fixed in 2.5% glutaraldehyde and 2% paraformaldehyde in 0.1 M Sorenson's phosphate buffer (pH 7.40) for 15 min and centrifuged for 3–4 min to pellet cells. Fixative was decanted, and fresh primary fixative was added and left overnight. Samples were rinsed 2x in 0.1 M phosphate buffer for 15 min and fixed in 1% osmium tetroxide with 0.8% potassium ferricyanide in 0.1 M phosphate buffer for 2 h. Samples were then rinsed in phosphate buffer 2x for 15 min, rinsed in DI H<sub>2</sub>O 2x for 5 min, and dehydrated in a graded ethanol series. Samples were infiltrated with a 1:1 mixture of Spurr epoxy resin and 100% ethanol for 1 h, and subsequently placed resin overnight. Samples were placed in fresh resin in BEEM capsules and cured in a vacuum oven at 70°C for 8 h. Samples were cut in 90 nm sections on a Leica (Wetzlar, Germany) UC7 ultramicrotome, and sections were collected on 200 mesh Formvar-coated copper grids. Grids were stained with 50% uranyl acetate in ethanol for 15 min, rinsed in DI H<sub>2</sub>O and stained with lead citrate for 15 min. Imaging was performed in bright field mode on a FEI Tecnai 12 Spirit transmission electron microscope with an accelerated voltage of 80keV. Ten images were collected for each sample ( $n=3$ ), and images were analyzed by point counting using a 15  $\mu\text{m}^2$  grid overlay in FIJI.

### Metabolic flux analysis

Mitochondrial function was evaluated in cells for both metformin and  $\beta$ -GPA 48-h treatment groups, as the mitochondrial electron transport system is a proposed target of metformin, and  $\beta$ -GPA has been shown to alter oxygen consumption rate *in vivo*. Cells were cultured as described above and seeded at a density of 6,000 cells per well into Seahorse XFp 8-well microplate cartridges. The only difference from the previously described culture methods is that 45 min prior to measurement, the media was replaced with Seahorse XFp culture media, supplemented with 25 mM glucose, 1 mM pyruvate and 2 mM glutamine. This supplemented media has the same composition as the DMEM culture media used in the rest of this study, with the exception that there is no sodium-bicarbonate, which would interfere with the measurements of pH. To prevent acidification from occurring in this non-buffered media, the cells were maintained in a non-CO<sub>2</sub> incubator for the final 45 min prior to the experiments.

Two of the 8 wells of the microplate cartridge were used as calibration controls, containing only media, and six wells contained cells; three controls and three treatment wells. Experiments were conducted in triplicate for a total of nine replicates per treatment. Prior to and after each experiment the wells were examined microscopically. In all cases, a confluent layer of cells was observed for both treatments before and after the experiment, with a

mixture of myocytes and myotubes like that shown for the 48-h treatment in Fig. 1 A and D. To account for the possibility that the treatments affected total cell density, all measurements were normalized to total protein.

The cellular oxygen consumption rate (OCR) was measured in a Seahorse XFp metabolic flux analyzer (Seahorse Bioscience, North Billerica, MA, USA). To evaluate mitochondrial function, OCR was measured in the presence of (1) only media to obtain basal rates, (2) 1  $\mu\text{M}$  oligomycin to inhibit the ATP synthase and measure OCR from the mitochondrial proton leak + non-mitochondrial OCR, (3) 2  $\mu\text{M}$  FCCP to uncouple mitochondria and measure maximal OCR, and (4) 0.5  $\mu\text{M}$  rotenone/antimycin A to inhibit the electron transport system and measure only non-mitochondrial OCR. The OCR dedicated to different processes is calculated as follows: basal = initial OCR – non-mitochondrial OCR, maximal = post-FCCP OCR – non-mitochondrial OCR, ATP production = basal OCR – post-oligomycin OCR, proton leak = post-oligomycin OCR – non-mitochondrial OCR, and non-mitochondrial = post-rotenone/antimycin-A OCR. Basal OCR was collected for 3 time points, and 3 time points also were collected following each inhibitor injection (each time point is about 6 min, including mixing time). For the calculations described above, we used the OCR measurement at the third (last) time point under each condition to give the cells a chance to reach equilibrium (i.e., the 3<sup>rd</sup>, 6<sup>th</sup>, 9<sup>th</sup>, and 12<sup>th</sup> measurements were used). Simultaneous measurements of the extracellular acidification rate (ECAR), which is caused largely by anaerobic metabolism but also by aerobic CO<sub>2</sub> production, were also made. All data were analyzed using t-tests, and all data are presented as means  $\pm$  sem.

## Results

### $\beta$ -GPA and metformin alter myotube morphology

Myotubes treated with  $\beta$ -GPA were significantly longer and smaller in diameter than controls at 48 h, 72 h, 4 days, and 5 days (Fig. 1A, B). TEM revealed no significant response in cell size following 48 h  $\beta$ -GPA treatment (Fig. 1C). Myotubes treated with metformin were significantly larger in diameter, but only at the 48-h time point, and with no difference in length. Thus, controls and treatments were not morphologically different at 72 h, 4 days, or 5 days (Fig. 1D, E). This observation was further confirmed by TEM, where 48 h metformin treatment resulted in a 52.5% ( $P < 0.001$ ) increase in cell size (Fig. 1F). Phase contrast imaging revealed no significant differences in number of myotubes per field following either  $\beta$ -GPA or metformin treatment.

### 48 h treatment with $\beta$ -GPA and metformin increased AMPK activation

Both AMPK and ULK1 phosphorylation were investigated to determine the role of  $\beta$ -GPA and metformin on AMPK signaling and autophagy. Given that mTORC1 regulates autophagy in a reciprocal manner from AMPK, mTORC1 signaling was also evaluated. P70 S6 kinase (P70S6K) is a downstream target of mTORC1 and plays a role in regulation of protein synthesis.  $\beta$ -GPA treatment for 48 h significantly increased AMPK phosphorylation at Thr<sup>172</sup> ( $P < 0.05$ ), as well as phosphorylation of the autophagy initiating kinase ULK1 at Ser<sup>317</sup> ( $P < 0.05$ ). Phosphorylation of P70S6K was significantly reduced at Thr<sup>389</sup> ( $P < 0.05$ ), suggesting a reduction in mTORC1 signaling, consistent with increased AMPK activity and

autophagy induction (Fig. 2A). Metformin treatment induced phosphorylation of AMPK, but unlike  $\beta$ -GPA did not have an effect ULK1, or P70S6K phosphorylation (Fig. 2B).

### **$\beta$ -GPA and metformin differentially impacted autophagy in skeletal myotubes**

To further elucidate the role of  $\beta$ -GPA and metformin on autophagy, we used confocal microscopy to analyze LC3b-II and lysosome staining, TEM to evaluate autophagosome density and ultrastructure, and western blotting to determine protein expression of LC3b-II. Confocal microscopy revealed that 48 h  $\beta$ -GPA treatment induced a 66% increase in autophagosome (LC3b-II) density ( $P<0.001$ ) and a 67% increase in lysosome density ( $P<0.05$ ) (Fig. 3A, B). Total area of LC3b-II puncta was also investigated using a threshold analysis and was found to be significantly increased (53%;  $P<0.05$ ) in  $\beta$ -GPA treated cells. TEM complemented these findings, revealing a 3-fold increase in autophagosome density ( $P<0.001$ ) and 7-fold increase in autolysosome density ( $P<0.001$ ) (Fig. 3C, D). However, western blot analysis revealed no significant difference in LC3b-II expression (Fig. 3E).

In contrast to  $\beta$ -GPA, confocal microscopy revealed a significant reduction in autophagy following metformin treatment, marked by a 29% reduction in autophagosomes (LC3b-II) ( $P<0.01$ ) and a 55% reduction in lysosomes ( $P<0.05$ ) (Fig. 4A, B). Total area of LC3b-II puncta was also significantly reduced ( $P=0.01$ ). TEM analysis revealed a 3-fold reduction in autophagosome density ( $P<0.001$ ) and no significant change in autolysosome density (Fig. 4C, D). Further, western blot analysis showed that metformin significantly reduced LC3b-II expression ( $P<0.05$ ) (Fig. 4E). Neither  $\beta$ -GPA nor metformin treatment elicited a significant difference in co-localization of LC3b-II and lysosomes ( $P=0.135$  and  $P=0.190$ , respectively).

### **$\beta$ -GPA and metformin decreased mitochondrial respiration**

To evaluate mitochondrial function, oxygen consumption rate (OCR) and extracellular acidification rate (ECAR) were measured during the injection of inhibitors following 48 h of  $\beta$ -GPA or metformin treatment (Fig. 5A–D).  $\beta$ -GPA led to significant reductions to basal ( $P<0.05$ ) and maximal OCR ( $P<0.05$ ), as well as non-mitochondrial OCR ( $P<0.05$ ) (Fig. 5E). Metformin, a known electron transport inhibitor, led to a more substantial reduction in OCR, and a significant decrease in basal ( $P<0.01$ ) and maximal OCR ( $P<0.01$ ), as well as the OCR devoted to ATP production ( $P<0.01$ ) and non-mitochondrial OCR ( $P<0.01$ ) (Fig. 5F).  $\beta$ -GPA reduced ECAR after FCCP injection, suggesting that total metabolic rate (aerobic and anaerobic) is lower following  $\beta$ -GPA treatment (Fig. 5C). In contrast, metformin caused a chronically high ECAR that was greater than the controls for all time points except when control ECAR was maximal during FCCP-induced uncoupling (Fig. 5D). This is consistent with metformin acting as a potent inhibitor of the electron transport system, and cellular recruitment of anaerobic glycolysis to compensate for the deficit in ATP production by mitochondria.

### **$\beta$ -GPA and metformin differentially altered mitochondrial morphology**

$\beta$ -GPA increases mitochondrial biogenesis *in vivo* (Bergeron, et al. 2001), and metformin has been shown to alter mitochondrial morphology (Izzo, et al. 2017). As such, mitochondrial morphology was investigated using transmission electron microscopy. 48 h  $\beta$ -GPA treatment led to a 40% increase in the density of fragmented mitochondria ( $P<0.05$ ),



with no change in elongated mitochondrial density (Fig. 6A, B). Metformin, in contrast, increased the density of elongated mitochondria by 84% ( $P < 0.001$ ), with no change in the density of fragmented mitochondria (Fig. 6C, D). Total mitochondrial density was not altered by  $\beta$ -GPA or metformin, which is not surprising for the relatively short 48 h treatment period.

## Discussion

The aim of this study was to determine how the anti-hyperglycemic drug metformin and the creatine analog  $\beta$ -GPA affect cell morphology, AMPK signaling, autophagy, and mitochondrial morphology and function in developing skeletal myotubes.  $\beta$ -GPA has been shown to reduce skeletal muscle mass and myofiber diameter *in vivo*, and this has been attributed to a shift toward more aerobic fiber types that are typically smaller to promote adequate diffusive flux of oxygen (Ross, et al. 2017). While most investigations of  $\beta$ -GPA have been primarily focused on *in vivo* experiments, some work has examined the morphological effects of  $\beta$ -GPA in cultured myoblasts. Ohira et al. (2011) discovered that adding 1 mM  $\beta$ -GPA near the end of myogenic differentiation did not alter myotube diameter or number of myotubes per field. Nickenko et al. (2016) found that 1 mM  $\beta$ -GPA treatment throughout differentiation led to a significant increase in the number of myotubes per field. In contrast to Ohira et al. (2011) and Nickenko et al. (2016), the present study found that myoblasts treated with  $\beta$ -GPA throughout differentiation were longer and smaller in diameter each day from 48 h to 5 days, with no change in the number of myotubes per field. The cell volume density results obtained by TEM were non-significant and did not reflect those obtained by phase contrast, possibly due to difficulty imaging entire cells and the much smaller sample size analyzed with TEM. Metformin treated cells were larger in diameter at 48 h, with no change in length or diameter at any other time point. This is consistent with Pavlidou et al. (2017), who found that the effects of metformin on myogenic differentiation was dose dependent, with low doses (100  $\mu$ M and 500  $\mu$ M, which is similar to the 1 mM dose in the present study) having no effect on differentiation. Neither  $\beta$ -GPA nor metformin treatment altered the number of myotubes per field (Fig. 1). Thus,  $\beta$ -GPA and metformin alter myotube shape in different ways, but the mechanisms of these effects are unclear.

$\beta$ -GPA supplementation has been shown to reduce ATP content in skeletal muscle, leading to subsequent increases in AMPK activity (Bergeron, et al. 2001; Rush, Tullson, and Terjung 1998; Zong, et al. 2002). In cultured muscle cells, one study reported no effect of  $\beta$ -GPA treatment on AMPK phosphorylation (Hanke, et al. 2008), while another study found AMPK activity was significantly reduced following  $\beta$ -GPA treatment (Ohira, et al. 2011). In the present study,  $\beta$ -GPA treatment significantly increased phosphorylation of AMPK, which was associated with increased ULK1 phosphorylation and reduced phosphorylation of P70S6K (Fig. 2A–C), which are results consistent with AMPK-induced enhancement of autophagy and inhibition of protein synthesis. P70S6K is a downstream target of mTORC1, which inhibits autophagy by inactivating the ULK1 complex (Hosokawa, et al. 2009). Further, P70S6K phosphorylates the ribosomal protein S6, thereby activating protein synthesis (Gingras, Raught, and Sonenberg 2001). Thus, the reduced P70S6K phosphorylation is expected to lead to reduced protein synthesis, and

enhanced phosphorylation of ULK1 is indicative of increased autophagy, both of which are consistent with the observed increase in AMPK phosphorylation. These results are in agreement with our findings that  $\beta$ -GPA treatment led to increased autophagosome, autolysosome, and lysosome density (Fig. 3A–D). In contrast, protein expression of LC3b-II was not altered (Fig. 3E). This could have resulted from increased autophagosome synthesis and degradation, *i.e.*, LC3b-II was rapidly turned over, as evidenced by the 7-fold increase in autolysosome density. These results in myotubes are consistent with those of Yang et al. (Yang, et al. 2015), where  $\beta$ -GPA was shown to increase AMPK signaling and autophagy in *Drosophila*.

Metformin has been shown to increase AMPK phosphorylation in hepatocytes and myocytes (Musi, et al. 2002; Zhou, et al. 2001), while Pavlidou et al. (2017) found that low doses of metformin did not lead to alterations in AMPK activity. The 48-h metformin treatment in the present study increased phosphorylation of AMPK but had no effect on ULK1 or P70S6K (Fig. 2D–F). If metformin had led to the expected changes in ULK1 and P70S6K phosphorylation, then we would also expect an upregulation of autophagy similar to that caused by  $\beta$ -GPA. Metformin, however, had the opposite effect on autophagy, suggesting a non-AMPK mediated mechanism. Studies assessing the effects of metformin on autophagy have focused primarily on cancer cells. In melanoma and lymphoma cells, metformin treatment has been shown to induce autophagy, although this was observed using high (5–10 mM) concentrations (Tomic, et al. 2011; Shi, et al. 2012). However, in micromolar concentrations, metformin has been shown to inhibit autophagy by decreasing glutamine metabolism and ammonia accumulation (Saladini, et al. 2019). Similarly, in the present study, a dose of 1 mM metformin led to a significant reduction in autophagy, evidenced by a dramatic reduction in LC3b-II expression, autophagosome density, and lysosome density (Fig. 4). In any case, the effect of metformin on autophagy activation is likely to be dose-dependent and cell-type specific.

Mitochondrial morphology, function, and degradation are impacted by cellular energy status and stress (Benard, et al. 2007; Yu, Robotham, and Yoon 2006; Melser, et al. 2013). In this study, both  $\beta$ -GPA and metformin reduced mitochondrial OCR, but the effect was greater for metformin (Fig. 5). The combined OCR and ECAR data suggest that overall metabolic rate is decreased in the  $\beta$ -GPA treated cells. This may reflect that  $\beta$ -GPA was inducing cellular remodeling toward a more aerobic phenotype, and metabolism is compromised during this period. This is consistent with *in vivo*  $\beta$ -GPA treatment, which leads to deterioration of exercise performance in the short-term while muscle remodeling occurs, but an enhancement of both metabolic rate and exercise performance in the long-term (Ross et al. 2017). The large effect of metformin on OCR is consistent with its role as an inhibitor of electron transport, as is the chronically high ECAR. The ECAR data suggests that anaerobic glycolysis is compensating for the decrease in ATP production by mitochondria in the metformin group. The fact that both the control and metformin groups reach the same ECAR following FCCP injection (when ECAR is maximal due to the combination of anaerobic glycolysis and aerobic CO<sub>2</sub> production) suggests that, unlike the  $\beta$ -GPA treatment, the overall ATP demand is the same in the control and metformin groups. The compromised mitochondria in the metformin treatment may be linked to changes in glutamine metabolism

and ammonium accumulation, as described above, which is a potential mechanism for the metformin-induced reduction in autophagy.

$\beta$ -GPA treatment also led to an increase in the density of fragmented mitochondria (Fig. 6). Mitochondrial fission precedes mitophagy (Gomes, Di Benedetto, and Scorrano 2011), so the sizable  $\beta$ -GPA-induced increase in autophagy observed in the present study may be associated with enhanced turnover of mitochondria. Further, *in vivo*  $\beta$ -GPA supplementation enhances AMPK activation, which can mimic the effects of exercise, including increases in mitochondrial biogenesis (Jager, et al. 2007). Exercise training favors mitochondrial fission, promoting mitophagy and aiding in the clearance of damaged or superfluous mitochondria, thereby improving mitochondrial quality (Yan, Lira, and Greene 2012; Lira, et al. 2013; Laker, et al. 2014; Drake, Wilson, and Yan 2016). However, mitochondrial fragmentation is also associated with mitochondrial dysfunction. Excess mitochondrial fission can result in accumulation of fragmented mitochondria, and is associated with diabetes related complications, such as diabetic cardiomyopathy and diabetes-induced atherosclerosis (Wang, et al. 2017; Toyama, et al. 2016).

Metformin treatment led to an increased density of elongated mitochondria. Metformin previously has been shown to promote mitochondrial elongation, restoring the mitochondrial network in fibroblasts (Izzo, et al. 2017). Metformin has also been reported to suppress mitochondrial fragmentation in an AMPK-dependent manner in endothelial cells, and inhibit the development of atherosclerosis in mice (Wang, et al. 2017). Moreover, elongated mitochondria are spared from autophagic degradation (Gomes, Di Benedetto, and Scorrano 2011), so the reduction in autophagy elicited by metformin may be associated with a reduction in mitophagy. In response to a variety of cellular stressors, some cell lines exhibit mitochondrial elongation, referred to as stress induced mitochondrial hyperfusion (Tondera, et al. 2009). In such situations, mitochondrial fusion allows mixing of matrix contents, and can thereby promote ATP production (Chan 2012). Given that metformin elicited a significant reduction in OCR associated with ATP production, mitochondrial elongation may have been a response to compensate for the reduction in ATP production and mitochondrial stress.

Obesity and T2D can cause perturbations in a whole host of cellular processes, including AMPK signaling, autophagy, and mitochondrial function (Kelley et al. 2002; Kosacka et al. 2015). In human skeletal muscle, obesity and T2D have been shown to elicit mitochondrial damage and mitochondrial size reduction (Kelley, et al. 2002). Further, while autophagy is essential for regular maintenance of skeletal muscle (Masiero, et al. 2009), alterations or reductions in skeletal muscle autophagy caused by obesity and T2D may lead to deleterious effects on muscle development, regeneration, and maintenance. Thus, agents that enhance autophagy and AMPK activity, such as  $\beta$ -GPA, may be potentially beneficial in the restoration of these cellular processes and therefore could have therapeutic implications for the treatment of these metabolic conditions. However, mitochondrial fragmentation, as observed in this study following  $\beta$ -GPA treatment, is associated with obesity, and may contribute to insulin resistance in skeletal muscle (Jheng, et al. 2012). Prior work has revealed increases in AMPK activity elicited by metformin treatment in hepatocytes and skeletal muscle (Zhou et al. 2001). While some studies have reported restoration of

AMPK activity and autophagy in response to metformin (Masini, et al. 2009; Xie, et al. 2011), the present study found that metformin activated AMPK, but led to a significant reduction in autophagy in cultured myocytes. It is well-established that metformin reduces hepatic glucose production and increases glucose disposal in skeletal muscle (Galuska et al. 1994; Foretz et al. 2010). However, the severe reduction in mitochondrial OCR and autophagy observed in the present study may impact skeletal muscle maintenance, thereby compromising the integrity of muscle fibers. As such, more work is required to evaluate the effects of  $\beta$ -GPA and metformin on skeletal muscle autophagy and mitochondrial maintenance in models of obesity and T2D.

In conclusion,  $\beta$ -GPA enhances autophagy and AMPK activity in developing C2C12 myotubes. This was accompanied by a reduction in myotube diameter, a decrease in basal and maximal OCR, and an increase the fragmented mitochondrial density. In contrast, metformin activated AMPK but led to a reduction in autophagy. Metformin also increased myotube diameter only at 48 h post-treatment, severely reduced basal and maximal OCR, and increased the density of elongated mitochondria. As autophagy and AMPK activation have been proposed as targets for the treatment of obesity and T2D, these results suggest that  $\beta$ -GPA could be beneficial for such metabolic conditions, despite the increase in mitochondrial fragmentation. While metformin is a widely used anti-hyperglycemic agent, the observed reduction in autophagy may lead to dysregulation of skeletal muscle maintenance, since basal autophagy is required to maintain skeletal muscle mass. Currently, more work is needed to further elucidate the effects of obesity and T2D on basal autophagy in skeletal muscle. To expand on the present study, future work should focus on how  $\beta$ -GPA and metformin influence mitochondrial fission and fusion machinery, and how these agents effect autophagy and insulin sensitivity *in vivo*.

## Acknowledgments

Financial support was provided by the National Institute of Diabetes and Digestive and Kidney Diseases of the National Institutes of Health (R15-DK106688).

## References

- Baumgarner BL, Nagle AM, Quinn MR, Farmer AE, Kinsey ST (2015) Dietary Supplementation of Beta-Guanidinopropionic Acid (Beta Gpa) Reduces Whole-Body and Skeletal Muscle Growth in Young Cd-1 Mice. *Molecular and Cellular Biochemistry* 403, no. 1–2 (5): 277–285. 10.1007/s11010-015-2357-7. [PubMed: 25701355]
- Benard G, Bellance N, James D, Parrone P, Fernandez H, Letellier T, Rossignol R (2007) Mitochondrial Bioenergetics and Structural Network Organization. *Journal of Cell Science* 120, no. 5 (3): 838–848. 10.1242/jcs.03381. [PubMed: 17298981]
- Bereiterhahn J, Voth M (1994) Dynamics of Mitochondria in Living Cells - Shape Changes, Dislocations, Fusion, and Fission of Mitochondria. *Microscopy Research and Technique* 27, no. 3 (2): 198–219. 10.1002/jemt.1070270303. [PubMed: 8204911]
- Bergeron R, Ren JM, Cadman KS, Moore IK, Perret P, Pypaert M, Young LH, Semenkovich CF, Shulman GI (2001) Chronic Activation of Amp Kinase Results in Nrf-1 Activation and Mitochondrial Biogenesis. *American Journal of Physiology-Endocrinology and Metabolism* 281, no. 6 (12): E1340–E1346. [PubMed: 11701451]
- Chan DC (2006) Mitochondria: Dynamic Organelles in Disease, Aging, and Development. *Cell* 125, no. 7 (6): 1241–1252. 10.1016/j.cell.2006.06.010. [PubMed: 16814712]

- Chan DC (2012) Fusion and Fission: Interlinked Processes Critical for Mitochondrial Health. In Annual Review of Genetics, Vol 46, vol 46, Annual Review of Genetics, 265–287.
- Cusi K, DeFronzo RA (1998) Metformin: A Review of Its Metabolic Effects. Diabetes Reviews 6, no. 2: 89–131.
- Drake JC, Wilson RJ, Yan Z (2016) Molecular Mechanisms for Mitochondrial Adaptation to Exercise Training in Skeletal Muscle. FASEB Journal 30, no. 1 (1): 13–22. 10.1096/fj.15-276337. [PubMed: 26370848]
- Egan DF, Kim J, Shaw RJ, Guan KL (2011) The Autophagy Initiating Kinase Ulk1 Is Regulated Via Opposing Phosphorylation by Ampk and Mtor. Autophagy 7, no. 6 (6): 645–646. 10.4161/autophagy.7.6.15123. [PubMed: 21460623]
- El-Mir MY, Nogueira V, Fontaine E, Averet N, Rigoulet M, Leverve X (2000) Dimethylbiguanide Inhibits Cell Respiration Via an Indirect Effect Targeted on the Respiratory Chain Complex I. Journal of Biological Chemistry 275, no. 1 (1): 223–228. 10.1074/jbc.275.1.223.
- Fitch CD, Jellinek M, Fitts RH, Baldwin KM, Holloszy JO (1975) Phosphorylated Beta-Guanidinopropionate as a Substitute for Phosphocreatine in Rat Muscle. American Journal of Physiology 228, no. 4: 1123–1125.
- Fitch CD, Jellinek M, Mueller EJ (1974) Experimental Depletion of Creatine and Phosphocreatine from Skeletal-Muscle. Journal of Biological Chemistry 249, no. 4: 1060–1063.
- Foretz M, Hebrard S, Leclerc J, Zarrinpashneh E, Soty M, Mithieux G, Sakamoto K, Andreelli F, Viollet B (2010) Metformin Inhibits Hepatic Gluconeogenesis in Mice Independently of the Lkb1/Ampk Pathway Via a Decrease in Hepatic Energy State. Journal of Clinical Investigation 120, no. 7 (7): 2355–2369. 10.1172/JCI40671.
- Fryer LGD, Parbu-Patel A, Carling D (2002) The Anti-Diabetic Drugs Rosiglitazone and Metformin Stimulate Amp-Activated Protein Kinase through Distinct Signaling Pathways. Journal of Biological Chemistry 277, no. 28 (7): 25226–25232. 10.1074/jbc.M202489200.
- Galuska D, Nolte LA, Zierath JR, Wallberghenriksson H (1994) Effect of Metformin on Insulin-Stimulated Glucose-Transport in Isolated Skeletal-Muscle Obtained from Patients with Niddm. Diabetologia 37, no. 8 (8): 826–832. 10.1007/BF00404340. [PubMed: 7988785]
- Ganley IG, Lam DH, Wang JR, Ding XJ, Chen S, Jiang XJ (2009) Ulk1 Center Dot Atg13 Center Dot Fip200 Complex Mediates Mtor Signaling and Is Essential for Autophagy. Journal of Biological Chemistry 284, no. 18 (5): 12297–12305. 10.1074/jbc.M900573200.
- Gingras AC, Raught B, Sonenberg N (2001) Regulation of Translation Initiation by Frap/Mtor. Genes & Development 15, no. 7 (4): 807–826. 10.1101/gad.887201. [PubMed: 11297505]
- Gomes LC, Di Benedetto G, Scorrano L (2011) During Autophagy Mitochondria Elongate, Are Spared from Degradation and Sustain Cell Viability. Nature Cell Biology 13, no. 5 (5): 589–U207. 10.1038/ncb2220. [PubMed: 21478857]
- Gwinn DM, Shackelford DB, Egan DF, Mihaylova MM, Mery A, Vasquez DS, Turk BE, Shaw RJ (2008) Ampk Phosphorylation of Raptor Mediates a Metabolic Checkpoint. Molecular Cell 30, no. 2 (4): 214–226. 10.1016/j.molcel.2008.03.003. [PubMed: 18439900]
- Hanke N, Meissner JD, Scheibe RJ, Endeward V, Gros G, Kubis HP (2008) Metabolic Transformation of Rabbit Skeletal Muscle Cells in Primary Culture in Response to Low Glucose. Biochimica Et Biophysica Acta-Molecular Cell Research 1783, no. 5 (5): 813–825. 10.1016/j.bbamcr.2007.12.012.
- Hardie DG (2003) Minireview: The Amp-Activated Protein Kinase Cascade: The Key Sensor of Cellular Energy Status. Endocrinology 144, no. 12 (12): 5179–5183. 10.1210/en.2003-0982. [PubMed: 12960015]
- Hardie DG (2005) New Roles for the Lkb1 -> Ampk Pathway. Current Opinion in Cell Biology 17, no. 2 (4): 167–173. 10.1016/j.ceb.2005.01.006. [PubMed: 15780593]
- Hardie DG (2007) Amp-Activated/Snf1 Protein Kinases: Conserved Guardians of Cellular Energy. Nature Reviews Molecular Cell Biology 8, no. 10 (10): 774–785. 10.1038/nrm2249. [PubMed: 17712357]
- Hardie DG, Salt IP, Hawley SA, Davies SP (1999) Amp-Activated Protein Kinase: An Ultrasensitive System for Monitoring Cellular Energy Charge. Biochemical Journal 338 (3): 717–722. 10.1042/0264-6021:3380717.

- Hawley SA, Davison M, Woods A, Davies SP, Beri RK, Carling D, Hardie DG (1996) Characterization of the Amp-Activated Protein Kinase Kinase from Rat Liver and Identification of Threonine 172 as the Major Site at Which It Phosphorylates Amp-Activated Protein Kinase. *Journal of Biological Chemistry* 271, no. 44 (11): 27879–27887.
- Hay N, Sonenberg N (2004) Upstream and Downstream of Mtor. *Genes & Development* 18, no. 16 (8): 1926–1945. 10.1101/gad.1212704.
- Holmes BF, Kurth-Kraczek EJ, Winder WW (1999) Chronic Activation of 5'-Amp-Activated Protein Kinase Increases Glut-4, Hexokinase, and Glycogen in Muscle. *Journal of Applied Physiology* 87, no. 5 (11): 1990–1995. [PubMed: 10562646]
- Hosokawa N, Hara T, Kaizuka T, Kishi C, Takamura A, Miura Y, Iemura S, Natsume T, Takehana K, Yamada N, Guan JL, Oshiro N, Mizushima N (2009) Nutrient-Dependent Mtorc1 Association with the Ulk1-Atg13-Fip200 Complex Required for Autophagy. *Molecular Biology of the Cell* 20, no. 7 (4): 1981–1991. 10.1091/mbc.E08-12-1248. [PubMed: 19211835]
- Hundal RS, Krssak M, Dufour S, Laurent D, Lebon V, Chandramouli V, Inzucchi SE, Schumann WC, Petersen KF, Landau BR, Shulman GI (2000) Mechanism by Which Metformin Reduces Glucose Production in Type 2 Diabetes. *Diabetes* 49, no. 12 (12): 2063–2069. 10.2337/diabetes.49.12.2063. [PubMed: 11118008]
- Hutber CA, Hardie DG, Winder WW (1997) Electrical Stimulation Inactivates Muscle Acetyl-Coa Carboxylase and Increases Amp-Activated Protein Kinase. *American Journal of Physiology-Endocrinology and Metabolism* 272, no. 2 (2): E262–E266.
- Iglesias MA, Ye JM, Frangioudakis G, Saha AK, Tomas E, Ruderman NB, Cooney GJ, Kraegen EW (2002) Aicar Administration Causes an Apparent Enhancement of Muscle and Liver Insulin Action in Insulin-Resistant High-Fat-Fed Rats. *Diabetes* 51, no. 10 (10): 2886–2894. 10.2337/diabetes.51.10.2886. [PubMed: 12351423]
- Izzo A, Nitti M, Mollo N, Paladino S, Procaccini C, Faicchia D, Cali G, Genesio R, Bonfiglio F, Cicatiello R, Polishchuk E, Polishchuk R, Pinton P, Matarese G, Conti A, Nitsch L (2017) Metformin Restores the Mitochondrial Network and Reverses Mitochondrial Dysfunction in Down Syndrome Cells. *Human Molecular Genetics* 26, no. 6 (3): 1056–1069. 10.1093/hmg/ddx016. [PubMed: 28087733]
- Jager S, Handschin C, Pierre J, Spiegelman BM (2007) Amp-Activated Protein Kinase (Ampk) Action in Skeletal Muscle Via Direct Phosphorylation of Pgc-1 Alpha. *Proceedings of the National Academy of Sciences of the United States of America* 104, no. 29 (7): 12017–12022. 10.1073/pnas.0705070104. [PubMed: 17609368]
- Jheng HF, Tsal PJ, Guo SM, Rua LH, Chang CS, Su IJ, Chang CR, Tsai YS (2012) Mitochondrial Fission Contributes to Mitochondrial Dysfunction and Insulin Resistance in Skeletal Muscle. *Molecular and Cellular Biology* 32, no. 2 (1): 309–319. 10.1128/MCB.05603-11. [PubMed: 22083962]
- Jung CH, Jun CB, Ro SH, Kim YM, Otto NM, Cao J, Kundu M, Kim DH (2009) Ulk-Atg13-Fip200 Complexes Mediate Mtor Signaling to the Autophagy Machinery. *Molecular Biology of the Cell* 20, no. 7 (4): 1992–2003. 10.1091/mbc.E08-12-1249. [PubMed: 19225151]
- Kabeya Y, Mizushima N, Uero T, Yamamoto A, Kirisako T, Noda T, Kominami E, Ohsumi Y, Yoshimori T (2000) Lc3, a Mammalian Homologue of Yeast Apg8p, Is Localized in Autophagosomal Membranes after Processing. *Embo Journal* 19, no. 21 (11): 5720–5728. 10.1093/emboj/19.21.5720.
- Kelley DE, He J, Menshikova EV, Ritov VB (2002) Dysfunction of Mitochondria in Human Skeletal Muscle in Type 2 Diabetes. *Diabetes* 51, no. 10 (10): 2944–2950. 10.2337/diabetes.51.10.2944. [PubMed: 12351431]
- Kim J, Klionsky DJ (2000) Autophagy, Cytoplasm-to-Vacuole Targeting Pathway, and Pexophagy in Yeast and Mammalian Cells. *Annual Review of Biochemistry* 69: 303–342. 10.1146/annurev.biochem.69.1.303.
- Kim J, Kundu M, Viollet B, Guan KL (2011) Ampk and Mtor Regulate Autophagy through Direct Phosphorylation of Ulk1. *Nature Cell Biology* 13, no. 2 (2): 132–U71. 10.1038/ncb2152. [PubMed: 21258367]
- Kim KH, Lee MS (2014) Autophagy-a Key Player in Cellular and Body Metabolism. *Nature Reviews Endocrinology* 10, no. 6 (6): 322–337. 10.1038/nrendo.2014.35.

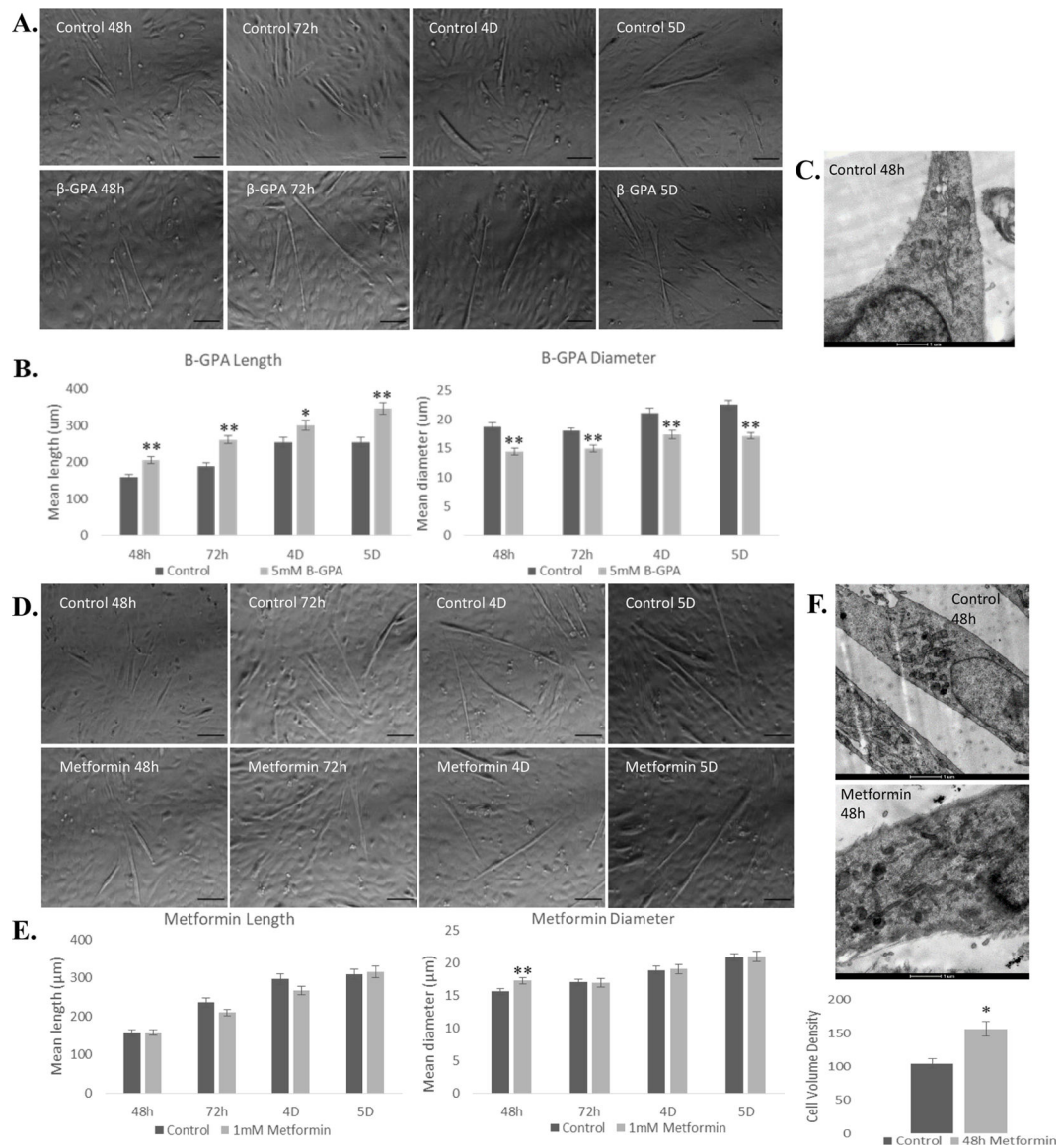
- Kurth-Kraczek EJ, Hirshman MF, Goodyear LJ, Winder WW (1999) 5' - Amp-Activated Protein Kinase Activation Causes Glut4 Translocation in Skeletal Muscle. *Diabetes* 48, no. 8 (8): 1667–1671. 10.2337/diabetes.48.8.1667. [PubMed: 10426389]
- Laker RC, Xu P, Ryall KA, Sujkowski A, Kenwood BM, Chain KH, Zhang M, Royal MA, Hoehn KL, Driscoll M, Adler PN, Wessells RJ, Saucerman JJ, Yan Z (2014) A Novel Mitotimer Reporter Gene for Mitochondrial Content, Structure, Stress, and Damage in Vivo. *Journal of Biological Chemistry* 289, no. 17 (4): 12005–12015. 10.1074/jbc.M113.530527.
- Laplante M, Sabatini DM (2009) An Emerging Role of Mtor in Lipid Biosynthesis. *Current Biology* 19, no. 22 (12): R1046–R1052. 10.1016/j.cub.2009.09.058. [PubMed: 19948145]
- Larsen S, Rabol R, Hansen CN, Madsbad S, Helge JW, Dela F (2012) Metformin-Treated Patients with Type 2 Diabetes Have Normal Mitochondrial Complex I Respiration. *Diabetologia* 55, no. 2 (2): 443–449. 10.1007/s00125-011-2340-0. [PubMed: 22009334]
- Lemasters JJ (2005) Perspective - Selective Mitochondrial Autophagy, or Mitophagy, as a Targeted Defense against Oxidative Stress, Mitochondrial Dysfunction, and Aging. *Rejuvenation Research* 8, no. 1 (Spr): 3–5. 10.1089/rej.2005.8.3. [PubMed: 15798367]
- Levine B, Klionsky DJ (2004) Development by Self-Digestion: Molecular Mechanisms and Biological Functions of Autophagy. *Developmental Cell* 6, no. 4 (4): 463–477. 10.1016/S1534-5807(04)00099-1. [PubMed: 15068787]
- Lira VA, Okutsu M, Zhang M, Greene NP, Laker RC, Breen DS, Hoehn KL, Yan Z (2013) Autophagy Is Required for Exercise Training-Induced Skeletal Muscle Adaptation and Improvement of Physical Performance. *Faseb Journal* 27, no. 10 (10): 4184–4193. 10.1096/fj.13-228486. [PubMed: 23825228]
- Masiero E, Agatea L, Mammucari C, Blaauw B, Loro E, Komatsu M, Metzger D, Reggiani C, Schiaffino S, Sandri M (2009) Autophagy Is Required to Maintain Muscle Mass. *Cell Metabolism* 10, no. 6 (12): 507–515. 10.1016/j.cmet.2009.10.008. [PubMed: 19945408]
- Masini M, Bugliani M, Lupi R, del Guerra S, Boggi U, Filipponi F, Marselli L, Masiello P, Marchetti P (2009) Autophagy in Human Type 2 Diabetes Pancreatic Beta Cells. *Diabetologia* 52, no. 6 (6): 1083–1086. 10.1007/s00125-009-1347-2. [PubMed: 19367387]
- Melser S, Chatelain EH, Lavie J, Mahfouf W, Jose C, Obre E, Goorden S, Priault M, Elgersma Y, Rezvani HR, Rossignol R, Benard G (2013) Rheb Regulates Mitophagy Induced by Mitochondrial Energetic Status. *Cell Metabolism* 17, no. 5 (5): 719–730. 10.1016/j.cmet.2013.03.014. [PubMed: 23602449]
- Merrill GF, Kurth EJ, Hardie DG, Winder WW (1997) Aica Riboside Increases Amp-Activated Protein Kinase, Fatty Acid Oxidation, and Glucose Uptake in Rat Muscle. *American Journal of Physiology-Endocrinology and Metabolism* 273, no. 6 (12): E1107–E1112.
- Morino K, Petersen KF, Shulman GI (2006) Molecular Mechanisms of Insulin Resistance in Humans and Their Potential Links with Mitochondrial Dysfunction. *Diabetes* 55 (12): S9–S15. 10.2337/db06-S002. [PubMed: 17130651]
- Musi N, Hirshman MF, Nygren J, Svanfeldt M, Bavenholm P, Rooyackers O, Zhou GC, Williamson JM, Ljunqvist O, Efendic S, Moller DE, Thorell A, Goodyear LJ (2002) Metformin Increases Amp-Activated Protein Kinase Activity in Skeletal Muscle of Subjects with Type 2 Diabetes. *Diabetes* 51, no. 7 (7): 2074–2081. 10.2337/diabetes.51.7.2074. [PubMed: 12086935]
- Oakhill JS, Steel R, Chen ZP, Scott JW, Ling N, Tam S, Kemp BE (2011) Ampk Is a Direct Adenylate Charge-Regulated Protein Kinase. *Science* 332, no. 6036 (6): 1433–1435. 10.1126/science.1200094. [PubMed: 21680840]
- Ohira Y, Kawano F, Roy RR, Edgerton VR (2003) Metabolic Modulation of Muscle Fiber Properties Unrelated to Mechanical Stimuli. *Japanese Journal of Physiology* 53, no. 6 (12): 389–400. 10.2170/jjphysiol.53.389.
- Ohira Y, Matsuoka Y, Kawano F, Ogura A, Higo Y, Ohira T, Terada M, Oke Y, Nakai N (2011) Effects of Creatine and Its Analog, Beta-Guanidinopropionic Acid, on the Differentiation of and Nucleoli in Myoblasts. *Bioscience Biotechnology and Biochemistry* 75, no. 6 (6): 1085–1089. 10.1271/bbb.100901.

- Ohira Y, Saito K, Wakatsuki T, Yasui W, Suetsugu T, Nakamura K, Tanaka H, Asakura T (1994) Responses of Beta-Adrenoceptor in Rat Soleus to Phosphorus Compound Levels and/or Unloading. *American Journal of Physiology* 266, no. 5 (5): C1257–C1262.
- Ota S, Horigome K, Ishii T, Nakai M, Hayashi K, Kawamura T, Kishino A, Taiji M, Kimura T (2009) Metformin Suppresses Glucose-6-Phosphatase Expression by a Complex I Inhibition and Ampk Activation-Independent Mechanism. *Biochemical and Biophysical Research Communications* 388, no. 2 (10): 311–316. 10.1016/j.bbrc.2009.07.164. [PubMed: 19664596]
- Pandke KE, Mullen KL, Snook LA, Bonen A, Dyck DJ (2008) Decreasing Intramuscular Phosphagen Content Simultaneously Increases Plasma Membrane Fat/Cd36 and Glut4 Transporter Abundance. *American Journal of Physiology-Regulatory Integrative and Comparative Physiology* 295, no. 3 (9): R806–R813. 10.1152/ajpregu.90540.2008.
- Pavlidou T, Rosina M, Fuoco C, Gerini G, Gargioli C, Castagnoli L, Cesareni G (2017) Regulation of myoblast differentiation by metabolic perturbations induced by metformin. *Plos One* 12 doi 10.1371/journal.pone.0182475
- Ren JM, Ohira Y, Holloszy JO, Hamalainen N, Traub I, Pette D (1995) Effects of Beta-Guanidinopropionic Acid-Feeding on the Patterns of Myosin Isoforms in Rat Fast-Twitch Muscle. *Pflugers Archiv-European Journal of Physiology* 430, no. 3 (7): 389–393. 10.1007/BF00373914. [PubMed: 7491263]
- Rena G, Hardie DG, Pearson ER (2017) The Mechanisms of Action of Metformin. *Diabetologia* 60, no. 9 (9): 1577–1585. 10.1007/s00125-017-4342-z. [PubMed: 28776086]
- Reznick RM, Shulman GI (2006) The Role of Amp-Activated Protein Kinase in Mitochondrial Biogenesis. *Journal of Physiology-London* 574, no. 1 (7): 33–39. 10.1113/jphysiol.2006.109512.
- Reznick RM, Zong HH, Li J, Morino K, Moore IK, Yu HJ, Liu ZX, Dong JY, Mustard KJ, Hawley SA, Befroy D, Pypaert M, Hardie DG, Young LH, Shulman GI (2007) Aging-Associated Reductions in Amp-Activated Protein Kinase Activity and Mitochondrial Biogenesis. *Cell Metabolism* 5, no. 2 (2): 151–156. 10.1016/j.cmet.2007.01.008. [PubMed: 17276357]
- Ross TT, Overton JD, Houmard KF, Kinsey ST (2017) Beta-Gpa Treatment Leads to Elevated Basal Metabolic Rate and Enhanced Hypoxic Exercise Tolerance in Mice. *Physiological Reports* 5, no. 5 (3). 10.14814/phy2.13192.
- Roussel D, Lhenry F, Ecochard L, Sempore B, Rouanet JL, Favier R (2000) Differential Effects of Endurance Training and Creatine Depletion on Regional Mitochondrial Adaptations in Rat Skeletal Muscle. *Biochemical Journal* 350 (9): 547–553. 10.1042/0264-6021:3500547.
- Rubinsztein DC, Codogno P, Levine B (2012) Autophagy Modulation as a Potential Therapeutic Target for Diverse Diseases. *Nature Reviews Drug Discovery* 11, no. 9 (9): 709–U84. 10.1038/nrd3802. [PubMed: 22935804]
- Rush JWE, Tullson PC, Terjung RL (1998) Molecular and Kinetic Alterations of Muscle Amp Deaminase During Chronic Creatine Depletion. *American Journal of Physiology-Cell Physiology* 274, no. 2 (2): C465–C471.
- Saladini S, Avenaggiato M, Barreca F, Morgante E, Sansone L, Russo MA, Tafani M (2019) Metformin Impairs Glutamine Metabolism and Autophagy in Tumour Cells. *Cells* 8, no. 79: 1–22. <http://dx.doi.org/10.3390>.
- Schindelin J, Arganda-Carreras I, Frise E, Kaynig V, Longair M, Pietzsch T, Preibisch S, Rueden C, Saalfeld S, Schmid B, Tinevez JY, White DJ, Hartenstein V, Eliceiri K, Tomancak P, Cardona A (2012) Fiji: An Open-Source Platform for Biological-Image Analysis. *Nature Methods* 9, no. 7 (7): 676–682. 10.1038/NMETH.2019. [PubMed: 22743772]
- Shaw RJ, Lamia KA, Vasquez D, Koo SH, Bardeesy N, DePinho RA, Montminy M, Cantley LC (2005) The Kinase Lkb1 Mediates Glucose Homeostasis in Liver and Therapeutic Effects of Metformin. *Science* 310, no. 5754 (12): 1642–1646. 10.1126/science.1120781. [PubMed: 16308421]
- Shi WY, Xiao D, Wang L, Dong LH, Yan ZX, Shen ZX, Chen SJ, Chen Y, Zhao WL (2012) Therapeutic Metformin/Ampk Activation Blocked Lymphoma Cell Growth Via Inhibition of Mtor Pathway and Induction of Autophagy. *Cell Death & Disease* 3 (3). 10.1038/cddis.2012.13.



- Shields RP, Whitehair CK (1973) Muscle Creatine - in-Vivo Depletion by Feeding Beta-Guanidinopropionic Acid. *Canadian Journal of Biochemistry* 51, no. 7: 1046–1049. 10.1139/o73-136. [PubMed: 4725354]
- Shoubridge EA, Challiss RAJ, Hayes DJ, Radda GK (1985) Biochemical Adaptation in the Skeletal Muscle of Rats Depleted of Creatine with the Substrate-Analog Beta-Guanidinopropionic Acid. *Biochemical Journal* 232, no. 1: 125–131. 10.1042/bj2320125.
- Stephenne X, Foretz M, Taleux N, van der Zon GC, Sokal E, Hue L, Viollet B, Guigas B (2011) Metformin Activates Amp-Activated Protein Kinase in Primary Human Hepatocytes by Decreasing Cellular Energy Status. *Diabetologia* 54, no. 12 (12): 3101–3110. 10.1007/s00125-011-2311-5. [PubMed: 21947382]
- Stumvoll M, Haring HU, Matthaei S (2007) Metformin. *Endocrine Research* 32, no. 1–2: 39–57. 10.1080/07435800701743828. [PubMed: 18271504]
- Stumvoll M, Nurjhan N, Perriello G, Dailey G, Gerich JE (1995) Metabolic Effects of Metformin in Non-Insulin-Dependent Diabetes-Mellitus. *New England Journal of Medicine* 333, no. 9 (8): 550–554. 10.1056/NEJM199508313330903.
- Suwa M, Nakano H, Kumagai S (2003) Effects of Chronic Aicar Treatment on Fiber Composition, Enzyme Activity, Ucp3, and Pgc-1 in Rat Muscles. *Journal of Applied Physiology* 95, no. 3 (9): 960–968. 10.1152/japplphysiol.00349.2003. [PubMed: 12777406]
- Tomic T, Botton T, Cerezo M, Robert G, Luciano F, Puissant A, Gounon P, Allegra M, Bertolotto C, Bereder JM, Tartare-Deckert S, Bahadoran P, Auberger P, Ballotti R, Rocchi S (2011) Metformin Inhibits Melanoma Development through Autophagy and Apoptosis Mechanisms. *Cell Death & Disease* 2 (9). 10.1038/cddis.2011.86.
- Tondera D, Grandemange S, Jourdain A, Karbowski M, Mattenberger Y, Herzig S, Da Cruz S, Clerc P, Raschke I, Merkwirth C, Ehses S, Krause F, Chan DC, Alexander C, Bauer C, Youle R, Langer T, Martinou JC (2009) Slp-2 Is Required for Stress-Induced Mitochondrial Hyperfusion. *Embo Journal* 28, no. 11 (6): 1589–1600. 10.1038/emboj.2009.89.
- Toyama EQ, Herzig S, Courchet J, Lewis TL, Loson OC, Hellberg K, Young NP, Chen H, Polleux F, Chan DC, Shaw RJ (2016) Amp-Activated Protein Kinase Mediates Mitochondrial Fission in Response to Energy Stress. *Science* 351, no. 6270 (1): 275–281. 10.1126/science.aab4138. [PubMed: 26816379]
- Viollet B, Guigas B, Garcia NS, Leclerc J, Foretz M, Andreelli F (2012) Cellular and Molecular Mechanisms of Metformin: An Overview. *Clinical Science* 122, no. 5–6 (3): 253–270. 10.1042/cs20110386. [PubMed: 22117616]
- Wakatsuki T, Ohira Y, Nakamura K, Asakura T, Ohno H, Yamamoto M (1995) Changes of Contractile Properties of Extensor Digitorum Longus in Response to Creatine-Analogue Administration and/or Hindlimb Suspension in Rats. *Japanese Journal of Physiology* 45, no. 6: 979–989. 10.2170/jjphysiol.45.979.
- Wallimann T, Dolder M, Schlattner U, Eder M, Hornemann T, O’Gorman E, Ruck A, Brdiczka D (1998) Some New Aspects of Creatine Kinase (Ck): Compartmentation, Structure, Function and Regulation for Cellular and Mitochondrial Bioenergetics and Physiology. *Biofactors* 8, no. 3–4: 229–234. 10.1002/biof.5520080310. [PubMed: 9914824]
- Wang QL, Zhang M, Torres G, Wu SN, Ouyang CH, Xie ZL, Zou MH (2017) Metformin Suppresses Diabetes-Accelerated Atherosclerosis Via the Inhibition of Drp1-Mediated Mitochondrial Fission. *Diabetes* 66, no. 1 (1): 193–205. 10.2337/db16-0915. [PubMed: 27737949]
- Williams DB, Sutherland LN, Bomhof MR, Basaraba SAU, Thrush AB, Dyck DJ, Field CJ, Wright DC (2009) Muscle-Specific Differences in the Response of Mitochondrial Proteins to Beta-Gpa Feeding: An Evaluation of Potential Mechanisms. *American Journal of Physiology-Endocrinology and Metabolism* 296, no. 6 (6): E1400–E1408. 10.1152/ajpendo.90913.2008. [PubMed: 19318515]
- Williamson DL, Butler DC, Alway SE (2009) Ampk Inhibits Myoblast Differentiation through a Pgc-1 Alpha-Dependent Mechanism. *American Journal of Physiology-Endocrinology and Metabolism* 297, no. 2 (8): E304–E314. 10.1152/ajpendo.91007.2008. [PubMed: 19491292]
- Winder WW, Hardie DG (1996) Inactivation of Acetyl-Coa Carboxylase and Activation of Amp-Activated Protein Kinase in Muscle During Exercise. *American Journal of Physiology-Endocrinology and Metabolism* 270, no. 2 (2): E299–E304.

- Winder WW, Hardie DG (1999) Amp-Activated Protein Kinase, a Metabolic Master Switch: Possible Roles in Type 2 Diabetes. *American Journal of Physiology-Endocrinology and Metabolism* 277, no. 1 (7): E1–E10.
- Wullschleger S, Loewith R, Hall MN (2006) Tor Signaling in Growth and Metabolism. *Cell* 124, no. 3 (2): 471–484. 10.1016/j.cell.2006.01.016. [PubMed: 16469695]
- Xie ZL, Lau K, Eby B, Lozano P, He CY, Pennington B, Li HL, Rathi S, Dong YZ, Tian R, Kem D, Zou MH (2011) Improvement of Cardiac Functions by Chronic Metformin Treatment Is Associated with Enhanced Cardiac Autophagy in Diabetic Ove26 Mice. *Diabetes* 60, no. 6 (6): 1770–1778. 10.2337/db10-0351. [PubMed: 21562078]
- Yan Z, Lira VA, Greene NP (2012) Exercise Training-Induced Regulation of Mitochondrial Quality. *Exercise and Sport Sciences Reviews* 40, no. 3 (7): 159–164. [PubMed: 22732425]
- Yang S, Long LH, Li D, Zhang JK, Jin S, Wang F, Chen JG (2015) Beta-Guanidinopropionic Acid Extends the Lifespan of *Drosophila Melanogaster* Via an Amp-Activated Protein Kinase-Dependent Increase in Autophagy. *Aging Cell* 14, no. 6 (12): 1024–1033. 10.1111/accel.12371. [PubMed: 26120775]
- Yu TZ, Robotham JL, Yoon Y (2006) Increased Production of Reactive Oxygen Species in Hyperglycemic Conditions Requires Dynamic Change of Mitochondrial Morphology. *Proceedings of the National Academy of Sciences of the United States of America* 103, no. 8 (2): 2653–2658. 10.1073/pnas.0511154103. [PubMed: 16477035]
- Zhang BB, Zhou GC, Li C (2009) Ampk: An Emerging Drug Target for Diabetes and the Metabolic Syndrome. *Cell Metabolism* 9, no. 5 (5): 407–416. 10.1016/j.cmet.2009.03.012. [PubMed: 19416711]
- Zhou GC, Myers R, Li Y, Chen YL, Shen XL, Fenyk-Melody J, Wu M, Ventre J, Doebber T, Fujii N, Musi N, Hirshman MF, Goodyear LJ, Moller DE (2001) Role of Amp-Activated Protein Kinase in Mechanism of Metformin Action. *Journal of Clinical Investigation* 108, no. 8 (10): 1167–1174. 10.1172/JCI13505.
- Zong HH, Ren JM, Young LH, Pypaert M, Mu J, Birnbaum MJ, Shulman GI (2002) Amp Kinase Is Required for Mitochondrial Biogenesis in Skeletal Muscle in Response to Chronic Energy Deprivation. *Proceedings of the National Academy of Sciences of the United States of America* 99, no. 25 (12): 15983–15987. 10.1073/pnas.252625599. [PubMed: 12444247]

**Fig. 1.**

$\beta$ -GPA and metformin differentially alter myotube morphology. **A, B)**  $\beta$ -GPA increased myotube length and reduced myotube diameter each day throughout differentiation. Scale bar = 100  $\mu$ m. **C)** TEM (scale bar = 1  $\mu$ m revealed 48 h  $\beta$ -GPA treatment led to 16.5% reduction in mean cell volume, but this was not significant ( $P=0.139$ ). **D, E)** Metformin treatment increased myotube diameter at 48 h, with no significant difference in length or diameter at any other time point. **F)** TEM (scale bar = 1  $\mu$ m) complemented these findings, revealing a 52.5% increase in cell size.  $n=36$ ; \* $P$  0.05, \*\* $P$  0.01.

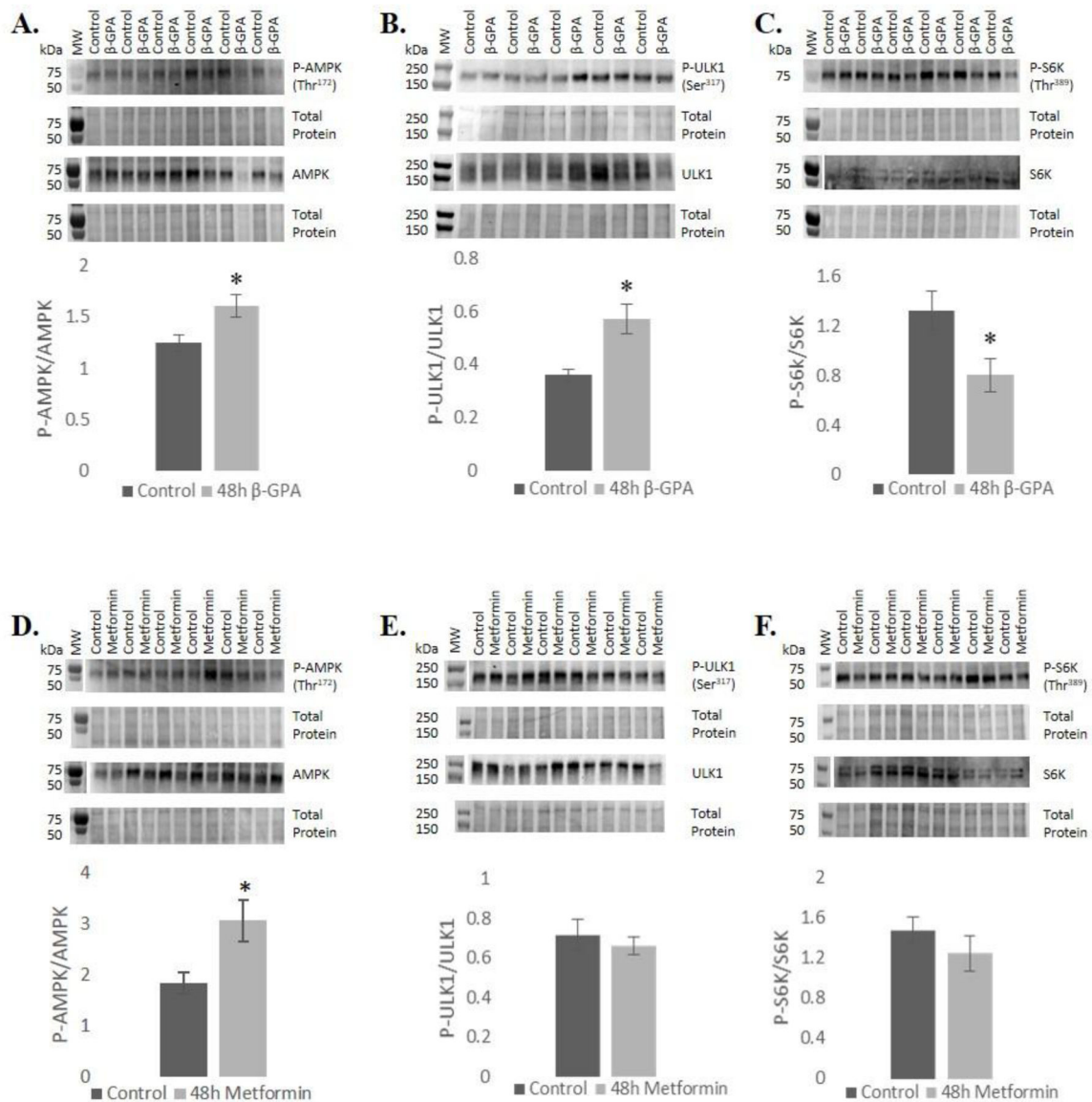


**Fig. 2.** 48 h  $\beta$ -GPA treatment led to an increase in phosphorylation of **A**) AMPK, reduced phosphorylation of **E**) P70S6K, and increased phosphorylation of **C**) ULK. Metformin led to increased phosphorylation of **D**) AMPK, but did not alter phosphorylation of **E**) P70S6K or **F**) ULK1. Molecular weight markers typically did not show up in the western blot ECL detection, so in those cases blots were aligned with total protein images and markers from total protein gels are shown adjacent to blots above and separated by a gap.  $n=6$  ( $n=9$  for control and metformin groups of AMPK); \* $P < 0.05$ .

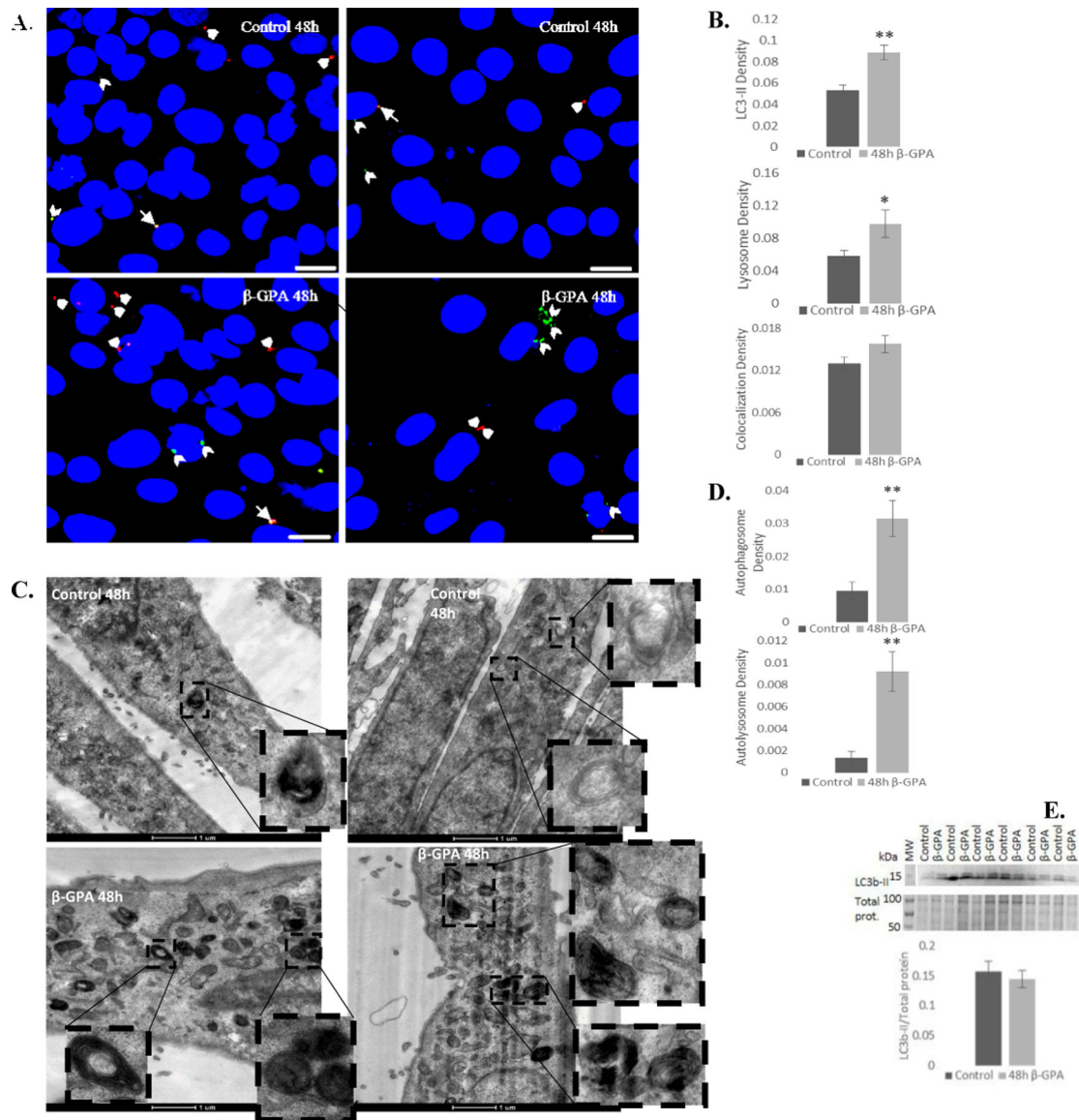


**Fig. 3.**  $\beta$ -GPA enhances autophagy in developing myotubes. **A, B)** Confocal microscopy revealed that  $\beta$ -GPA treatment led to an increase in autophagosome (green LC3-II labeling; beveled arrowheads) and lysosome (red lysotracker labeling; arrowheads) density, with no significant difference in colocalization (arrows) ( $n=45$ ). Scale bar = 20  $\mu$ m. **C, D)** TEM also revealed that 48h  $\beta$ -GPA increased autophagosome and autolysosome density ( $n=30$ ). **E)** 48 h  $\beta$ -GPA treatment did not alter relative expression of LC3b-II. There was insufficient total protein staining near the 15 kDa molecular weight marker, so LC3b-II was normalized to total protein from the 50–100 kDa range.  $n=6$ ; \*P 0.05, \*\* P 0.01.

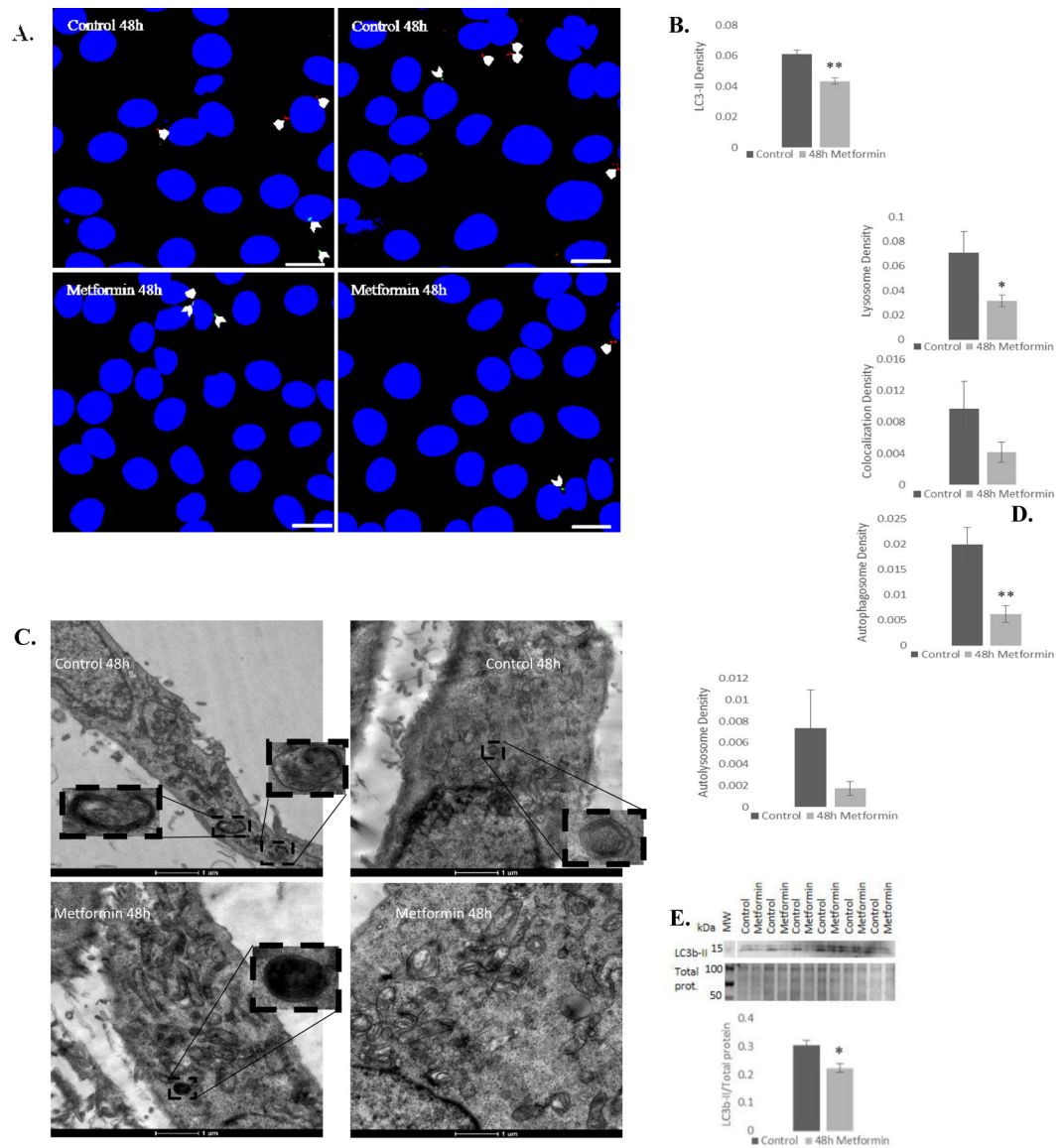


**Fig. 4.** Metformin reduces autophagy in developing myotubes. **A, B**) Confocal microscopy revealed that metformin treatment reduced autophagosome (green LC3-II labeling; beveled arrowheads) and lysosome (red lysotracker labeling; arrowheads) density, with no significant difference in colocalization (arrows) ( $n=45$ ). Scale bar = 20  $\mu\text{m}$ . **C, D**) TEM also revealed a reduction in autophagosome density ( $n=30$ ). **E**) Relative expression of LC3b-II was also reduced following metformin treatment. There was insufficient total protein staining near the 15 kDa molecular weight marker, so LC3b-II was normalized to total protein from the 50–100 kDa range.  $n=6$ ; \* $P$  0.05, \*\* $P$  0.01.

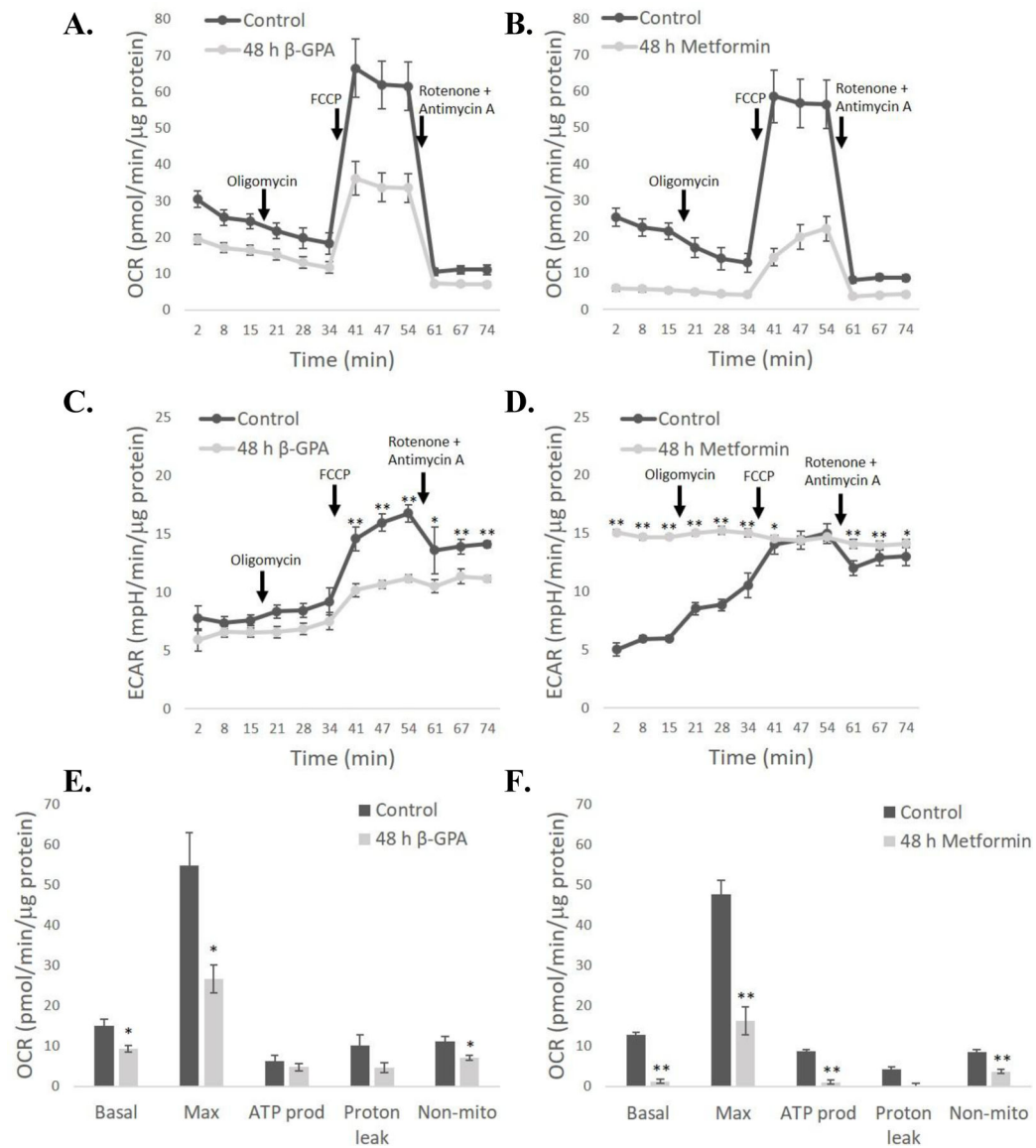


**Fig. 5.** Both  $\beta$ -GPA and metformin reduce mitochondrial oxygen consumption rate (OCR) in C2C12 cells. The time course of measurements of OCR and extracellular acidification rate (ECAR) are shown in **A-D**, while the allocation of OCR to different processes is shown in **E-F**. Mean OCR was reduced following both  $\beta$ -GPA **A, E**) and metformin treatment **C, D**). ECAR was reduced by  $\beta$ -GPA following addition of FCCP **C**), but metformin, a known inhibitor of the electron transport chain, led to chronically high ECAR that was significantly higher than controls for all time points except when FCCP was added and mitochondria were uncoupled **D**).  $n=9$ ; \*\*  $P$  0.01.

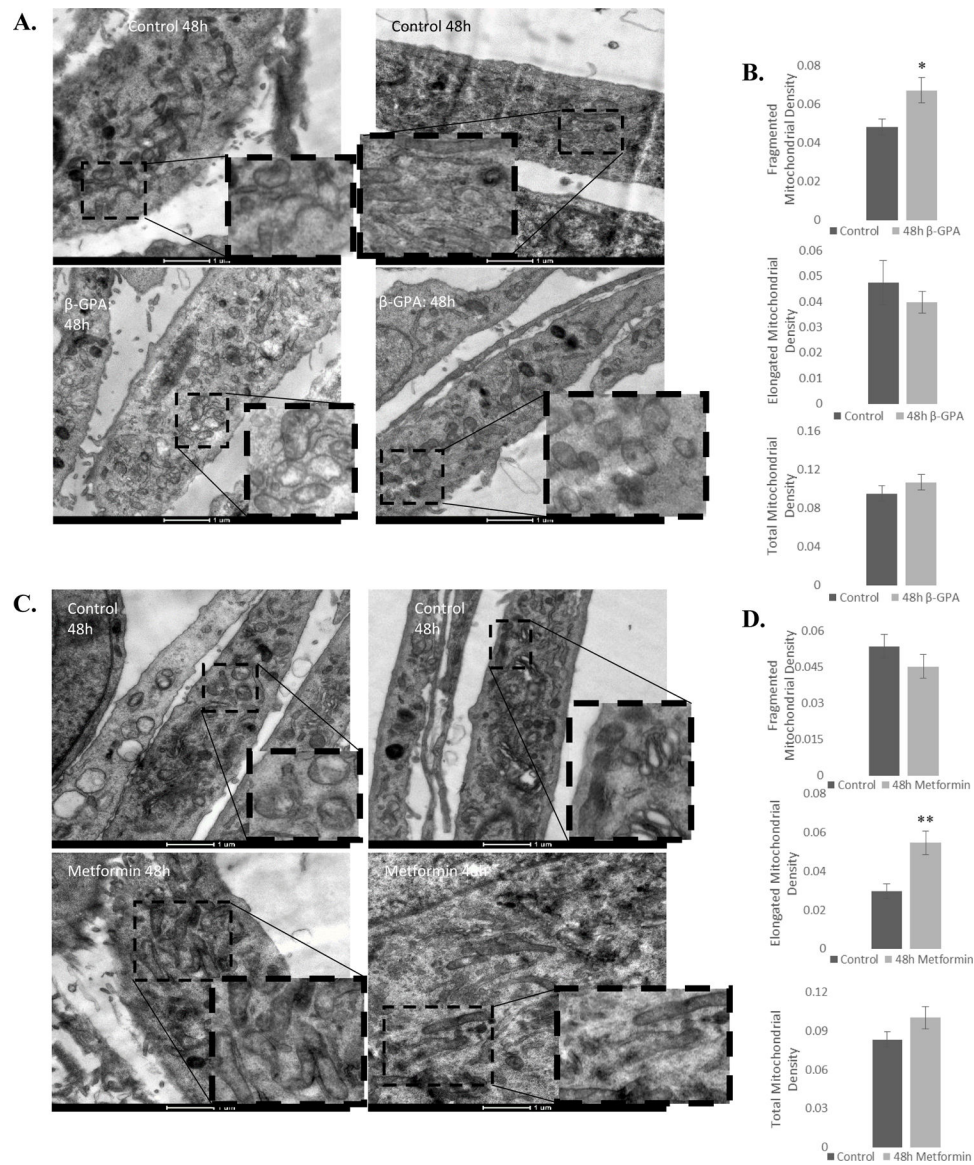


**Fig. 6.**  $\beta$ -GPA and metformin differentially alter mitochondrial morphology. **A, B)** 48 h  $\beta$ -GPA increased the density of fragmented mitochondria, and elicited no change in elongated mitochondria or total mitochondrial density. **C, D)** 48 h Metformin increased the density of elongated mitochondria, but did not alter the density of fragmented mitochondria, or total mitochondrial density.  $n=30$ ; \*P 0.05, \*\* P 0.01.